Available online at www.sciencedirect.com
SCIENCE DIRECT®
Spectrochimica Acta Part A 60 (2004) 3225–3232
SPECTROCHIMICA ACTA PART A
www.elsevier.com/locate/saa

Matrix isolation infrared and ab initio study of the hydrogen bonding between formic acid and water

Lisa George, Wolfram Sander*

Lehrstuhl für Organische Chemie II der Ruhr-Universität Bochum, Universitätsstr. 150, D44780 Bochum, Germany

Received 28 July 2003; accepted 11 March 2004

Abstract

The infrared spectra of the formic acid–water complexes isolated in argon matrices are reported. Both supersonic jet expansion and a conventional effusive source followed by trapping in solid argon at 10 K are used to obtain the matrices. The experimental IR spectra are compared to the data obtained from high level ab initio (MP2) and DFT (B3LYP) calculations with 6-311++G(d,p) and aug-cc-pVTZ basis sets. The complex formation results in red shifts in the C=O and O–H stretching vibrations and a blue shift in the C–O stretching vibration of formic acid. The O–H stretching modes of water also exhibit pronounced red shifts. Both the MP2 and B3LYP calculations located three minima corresponding to cyclic $HCOOH\cdots H_2O$ complexes with two hydrogen bond interactions. The binding energies are −10.3, −5.1, and −3.5 kcal mol^{-1}, respectively, for the three complexes at the MP2/ aug-cc-pVTZ level, corrected for the basis set superposition error (BSSE) using the Boys−Bernardi counterpoise scheme. Comparison of the calculated frequencies of the three complexes with the matrix IR spectrum reveals that the lowest energy complex is formed. In addition, a complex of formic acid with two water molecules is observed.

Keywords: Matrix isolation; Formic acid–water complexes; Infrared spectra; Ab initio calculations; Hydrogen bonding

1. Introduction

Hydrogen bonding interactions in molecular complexes are of theoretical [1–7] and experimental interest and were subject to numerous studies [5,8–12]. Rablen et al. calculated 53 hydrogen bonded complexes of water with various small organic molecules including alcohols, thiols, ethers, thioethers, carboxylic acids, esters, amines, amides, nitriles, and nitro compounds, using both B3LYP and MP2 theory [1].

Matrix isolation infrared spectroscopy in combination with ab initio theory has proven to be a powerful tool to characterize hydrogen bonding interactions. As the simplest carboxylic acid, formic acid is a prototype for investigating hydrogen bond interactions of acids in solvents to understand the microsolvation. A few theoretical studies of the structure of the complexes between formic acid and water were published [1,2,13–17]. In addition, two experimental studies of the formic acid–water complex using far infrared and microwave spectroscopy were reported [13,15]. Astrand et al. identified three structures of formic acid–water 1:1 complexes using the NEMO/ZPVE approach with binding energies of −9.2, −4.9, and −3.0 kcal mol^{-1}. They also reported the intermolecular modes in the far infrared spectrum of the complex in solid argon [13]. The rotational spectra and the ab initio characterization of formic acid–water complexes reported by Priem et al. revealed that the most stable structures with one and two water molecules are cyclic [15]. The most recent computational study of formic acid–water complexes at the B3LYP/6-311++G(d,p) level of theory located six minima corresponding to the *trans* and *cis* conformation of formic acid with 1–3 water molecules [2]. It was found that in all cases the most stable complex has a cyclic structure. Since a detailed experimental vibrational assignment of the formic acid–water system was not available, we here compare the matrix isolation infrared spectra of the complex of formic acid with 1–2 water molecules with high level computational results.

2. Experimental

Matrix isolation experiments were carried out by standard techniques using an APD CSW-202 Displex closed cycle

* Corresponding author. Tel.: +49-234-3228593; fax: +49-234-3214353.
E-mail address: wolfram.sander@ruhr-uni-bochum.de (W. Sander).

1386-1425/$ – see front matter © 2004 Elsevier B.V. All rights reserved.
doi:10.1016/j.saa.2004.03.004

helium cryostat, with both an effusive source for continuous deposition and a supersonic jet source for pulsed deposition. Formic acid was spectroscopic grade (Acros Organics), and water was of triply distilled quality and both samples were degassed several times by the freeze-pump-thaw method before mixing with argon. A glass mixing chamber was used for the effusive source, and a steel tank for the pulsed deposition with the supersonic jet source, using standard manometric methods. In continuous method of deposition, 0.5–2 mbar of formic acid was mixed with 1–5 mbar of water and diluted with 800 mbar of argon in a 2 l glass bulb. In the pulsed mode, 1–3 mbar of formic acid vapor was mixed with 2–5 mbar of water along with 1–2 bar of argon and equilibrated for 1–2 h before deposition. The argon mixed sample vapor was expanded through a pulsed nozzle and deposited on a CsI substrate held at 8 K. The pulse duration was varied between 300 μs and 5 ms, and a pulse frequency of 5 Hz was used. Deposition was done at 15 K for the continuous mode using effusive source. Matrices were annealed at 25 and 30 K by warming to this temperature for 15 min and cooling down to 8−10 K before recording the annealed spectra. In the pulsed deposition the temperature rise during the deposition resulted in complex formation without annealing. Spectra were recorded using Bruker Equinox 66v or IFS 66/s FTIR spectrometers at 0.5 cm^{-1} resolution.

3. Computational methods

Ab initio and DFT computations were performed using the Gaussian 98 program suite [18]. The equilibrium geometries and vibrational frequencies were calculated with the Møller−Plesset perturbation theory of second order (MP2) [19], and density functional theory (DFT) method with the B3LYP hybrid functional [20,21]. At both the MP2 and DFT level of calculations, a triple æ basis set added with diffuse functions and polarization functions (6-311++G(d,p)) [22,23], and also with Dunning's correlation consistent triple æ basis set [24], augmented with diffuse functions were used. To evaluate the effect of the basis set size, both Pople's and Dunning's basis sets were used at both the MP2 and DFT levels of theory. The stabilization energies were calculated at the MP2 level by subtracting the energies of the monomers from those of the complexes, and those energies were corrected for the basis set superposition errors (BSSE) using the counterpoise (CP) scheme of Boys and Bernardi [25]. The Gauss view program was used to visualize the molecular structure and vibrations, and the molecular structures were drawn with Povchem combined with Povray program.

4. Results and discussion

4.1. Experimental results

Infrared spectra of formic acid isolated in several rare gas matrices were reported earlier [26–31]. Vibrational modes

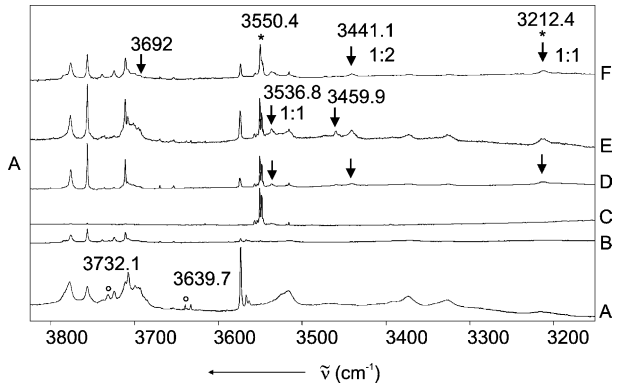

Fig. 1. Matrix isolation infrared spectra in the O–H stretching region of formic acid and the ν_3 and ν_1 stretching region of water: (A) H_2O–Ar (1/200); (B) H_2O–Ar (1/800, by supersonic jet sampling); (C) HCOOH–Ar (1/600); (D) HCOOH–H_2O–Ar (1/1/600); (E) HCOOH–H_2O–Ar (1/2/600); and (F) HCOOH–H_2O–Ar (1/1/800) by supersonic jet sampling. The ν_3 and ν_1 band origins marked by small circles and the formic acid monomer band marked by asterisk. The ν_3 and ν_1 band in the complex are marked by arrow and the ν_1 O–H stretch of formic acid in the complex are marked with arrow and asterisk. The peaks which are not marked are due to non-rotating monomer, dimer, and aggregates (see [36]).

corresponding to O–H, C=O, and C–O stretches are of main consideration for the molecular interaction studies of formic acid complexes. In order to identify the spectra of the formic acid–water complexes, infrared spectra of formic acid and water were recorded independently (using both the effusive and supersonic jet source for the deposition). The spectral resolution was found to be better with the supersonic jet source compared to the effusive source. The reference spectra of matrix-isolated formic acid [26,31] and water [32–37] are in good agreement with the spectra reported in the literature. New absorptions arising from the formation of formic acid−water complexes are shown in Figs. 1–3. Fig. 1 presents the O–H stretching region of formic acid and water. A and B correspond to the reference spectra of H_2O in

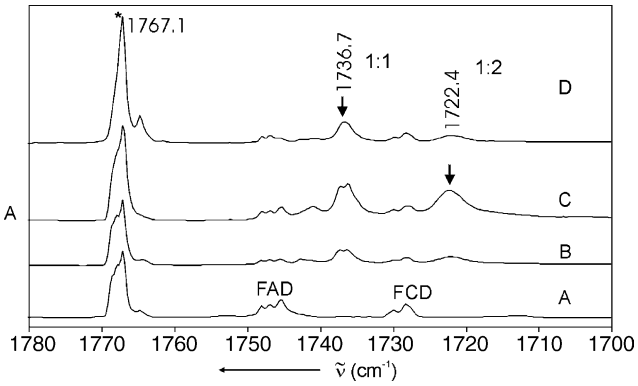

Fig. 2. Matrix isolation infrared spectra in the C=O stretching region of formic acid: (A) HCOOH–Ar (1/600); (B) HCOOH–H_2O–Ar (1/1/600); (C) HCOOH–H_2O–Ar (1/2/600); and (D) HCOOH–H_2O–Ar (1/1/1000) by supersonic jet sampling. FAD: formic acid acyclic dimer and FCD: formic acid cyclic dimer.

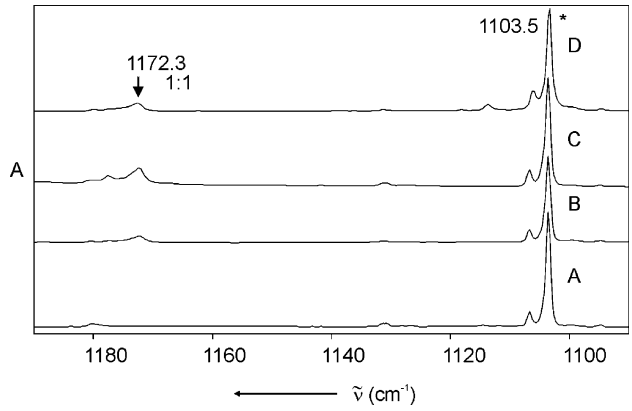

Fig. 3. Matrix isolation infrared spectra in the C–O stretching region of formic acid: (A) HCOOH–Ar (1/600); (B) HCOOH–H_2O–Ar (1/1/600); (C) HCOOH–H_2O–Ar (1/2/600); and (D) HCOOH–H_2O–Ar (1/1/1000) by supersonic jet sampling.

Ar obtained after continuous and supersonic jet deposition (1:200, annealed at 30 K and 1:800 at 8 K). The spectrum marked 'C' corresponds to a 1:600 molar ratio of formic acid and argon deposited at 15 K with subsequent annealing of the matrix at 30 K. The peak observed at 3550.4 cm^{-1} is assigned to the O–H stretching vibration of formic acid. The splitting of the band is attributed to site effects in the argon matrix [38]. Co-deposition of formic acid, water, and argon at a 1:1:600 molar ratio (D) results in a new absorption at 3212.4 cm^{-1}, red shifted by 338 cm^{-1} from the unperturbed OH mode of formic acid. On increasing the water concentration (E 1:2:600) the band at 3212.4 cm^{-1} gaines in intensity, revealing that this absorption is due to a formic acid–water complex (Fig. 1F). Even at low concentrations of formic acid and water this new peak appears, and hence it is assigned to a 1:1 complex of formic acid with water.

Due to rotating and non-rotating monomeric and dimeric species, matrix-isolated water exhibits many IR bands even at high dilutions, and the assignment of absorptions of complex absorptions in this region of the spectrum is thus difficult [36]. By variation of the water concentration and by annealing at higher temperatures (which allows the aggregation of matrix-isolated water via diffusion) new absorptions arising from complex formation are identified. In the water OH stretching region the formation of a complex with formic acid results in a new band around 3692 cm^{-1}, close to the ν_3 mode of water at 3734 cm^{-1} (3732.1 cm^{-1} after annealing the matrix at 30 K) (Fig. 1). The strong peak at 3712 cm^{-1} (rotating water monomer $1_{-1} \rightarrow 0_0$) [33] is broadened on annealing the matrix by overlapping with the H_2O dimer and multimer bands[36], and the complex absorption in fact seems to overlap with this broad band (D, E, and F). The difficulty of assigning absorptions arising from the formation of water complexes in this spectral region has been reported before [12].

The ν_1 mode of the water monomer was found as reported [34–36] at 3638 cm^{-1}, but on annealing the matrix with a higher water concentration ($Ar/H_2O = 200$) it is shifted to 3639.7 cm^{-1}. In the presence of formic acid, this band is red shifted by 103–3536.8 cm^{-1}. On increasing the formic acid concentration the intensity of the peak at 3536.8 cm^{-1} increases, and hence it is assigned to a perturbed ν_1 mode of water in the 1:1 complex of formic acid and water.

On annealing a diluted matrix at 25–30 K, two new bands are observed at 3441.1 and 3459.9 cm^{-1}. At higher water concentration (E, 1:2:600) and in the pulse deposition experiments these peaks appear even before annealing and are therefore tentatively assigned to a complex between formic acid and two water molecules (F). Fig. 2 displays the C=O stretching region of formic acid in four different experiments. The spectrum marked 'A' corresponds to a 1:600 molar ratio of formic acid and argon deposited at 15 K after annealing the matrix at 30 K. The peak at around 1767.1 cm^{-1} with a shoulder at 1764.8 cm^{-1} is assigned to the C=O stretching vibration of formic acid. The weak absorptions at around 1747 and 1728 cm^{-1} are assigned to the acyclic and cyclic forms of the formic acid dimer [31]. Even at high dilution of formic acid the dimer absorptions are observed. On co-deposition of formic acid, water, and argon (1:1:600 molar ratio) a new band appears at 1736.7 cm^{-1} (B). On increasing the water concentration, and also after annealing the matrix at 30 K, this band gains in intensity, revealing that it is due to a formic acid−water complex. The spectrum obtained by supersonic sampling is also given for comparison (D). Even at low concentrations of formic acid and water the peak at 1736.7 cm^{-1} appears, and therefore it is assigned to a perturbed C=O stretching mode of the 1:1 complex of formic acid and water. Another new band at 1722.4 cm^{-1} is observed on annealing the diluted matrix at 25–30 K. At higher water concentration (C, 1:2:600), this peak appears even before annealing, which indicates the interaction of formic acid with two water molecules. In pulsed deposition experiment, both the peaks appeared without annealing at lower concentrations as well (D). In the C–O stretching region of formic acid, a new distinct absorption is observed at 1172.3 cm^{-1} (Fig. 3B, C, and D), which is blue-shifted by 69 cm^{-1} from the unperturbed C–O stretching vibration of formic acid at 1103.5 cm^{-1}.

Experiments were carried out with D_2O to confirm the assignment of water modes arising from the formation of complexes. The shifts in the fundamental modes of formic acid in presence of D_2O are similar to that observed with H_2O. In addition, new bands are found due to a variety of complexes formed between formic acid and D_2O, HDO, and H_2O (Fig. 4).

4.2. Computational results

4.2.1. Structures and binding energies of the complexes

The structures of the formic acid−water complexes were calculated with ab-initio (MP2) and DFT (B3LYP) methods using both the aug-cc-pVTZ and 6-311++G(d,p) basis sets (Fig. 5). At all theoretical levels three minima corresponding to formic acid−water complexes are located on the po-

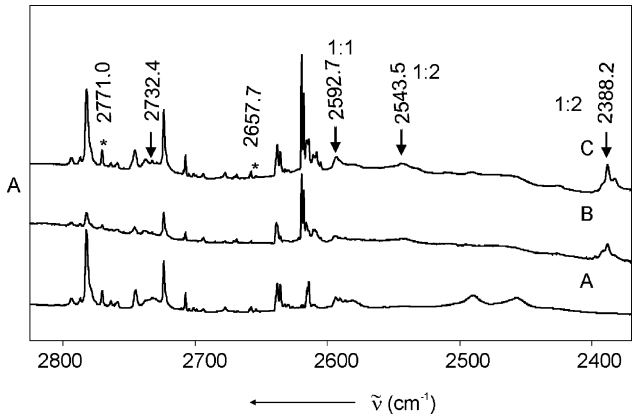

Fig. 4. Matrix isolation infrared spectra in the ν_3 and ν_1 stretching region of D_2O: (A) D_2O–Ar (1/300); (B) HCOOH–D_2O–Ar (1/1/600); and (C) HCOOH–D_2O–Ar (1/2/600). The ν_3 and ν_1 band origins of D_2O marked by asterisk and the complex peaks are marked by arrow. The peaks which are not marked are due to non-rotating monomer, dimer, and aggregates of D_2O and the ν_1 modes of HDO (see [36]).

tential energy surface. These structures resemble the three forms reported by Astrand et al. using the NEMO/ZPVE approach [13]. All three structures are planar at the MP2 level, but with B3LYP the planar structures give one imaginary frequency. Since the MP2 level with Dunning's basis set is considered to be more accurate to reproduce geometries and frequencies [39,40], our discussion is mainly based on the MP2 calculations.

In the global minimum structure A (Fig. 5), the main interaction is between the acidic hydrogen atom of formic acid and the oxygen atom of water. The second interaction is between one of the hydrogen atoms of water and the carbonyl oxygen atom of formic acid. The hydrogen bond distance for the first interaction is 1.768 and for the second interaction 2.002 Å (MP2/aug-cc-pVTZ), which indicates two strong interactions in the formic acid−water complex. These hydrogen bond distances agree well with the experimental data (1.810 and 2.210, respectively) [15]. The cyclic nature of the complex results in hydrogen bond angles of 157.6 and 136.2°, again close to the experimental values (160.8 and 120.3) [15].

Table 1
Calculated MP2 binding energies, raw, BSSE corrected, and ZPE corrected (in kcal mol^{-1}) of the formic acid–water complex

Complex	MP2/aug-cc-pVTZ			MP2/6-311G++(d,p)		
	ΔE	$\Delta E_{(BSSE)}$	$\Delta E_{(ZPE)}$	ΔE	$\Delta E_{(BSSE)}$	$\Delta E_{(ZPE)}$
A	−10.6	−10.3	−8.0	−10.4	−8.5	−7.9
B	−5.5	−5.1	−3.8	−5.3	−4.2	−3.6
C	−3.8	−3.5	−2.5	−4.1	−3.1	−2.6

The binding energy of complex A is −10.6 kcal mol^{-1} using MP2/aug-cc-pVTZ, in good agreement with the reported value (−10.7 kcal mol^{-1} at the MP2 = full/6-311++G(3df,2p)) [15]. After the BSSE correction the binding energy is reduced to −10.3 kcal mol^{-1} and after the ZPE correction (from 2.54 to −8.0 kcal mol^{-1}) (Table 1). The uncorrected binding energy obtained using MP2/6-311++G(d,p) is −10.4 kcal mol^{-1}. After the BSSE correction, the binding energy drops to −8.5 kcal mol^{-1} and after the ZPE correction, the binding energy is −7.9 kcal mol^{-1}. This result shows that for Dunning's correlation consistent basis set aug-cc-pVTZ the BSSE contribution is only small (0.3) compared to the total binding energy of the complex.

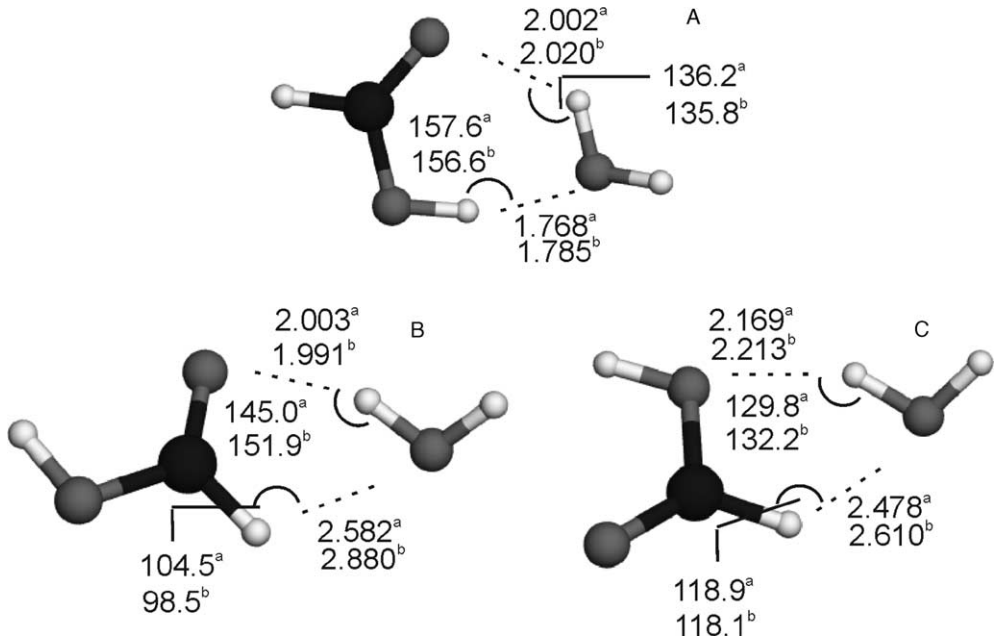

Fig. 5. The calculated structures of the 1:1 complexes A, B, and C of formic acid–water, with hydrogen bond lengths (Å) and hydrogen bond angles (°): [a]MP2/aug-cc-pVTZ; [b]B3LYP/aug-cc-pVTZ.

In structure B, the main interaction involves one hydrogen atom of water and the carbonyl oxygen atom of formic acid, and a secondary interaction in which the formyl hydrogen atom of formic acid interacts with the oxygen atom of water (Fig. 5). The hydrogen bond distances are 2.003 and 2.582 Å, respectively, at the MP2/aug-cc-pVTZ level. The hydrogen bond angles are non-linear, as expected for a cyclic structure. The binding energy is $-5.5\,\mathrm{kcal\,mol^{-1}}$ (MP2/aug-cc-pVTZ), which is reduced to $-5.1\,\mathrm{kcal\,mol^{-1}}$ after the BSSE correction and to $-3.8\,\mathrm{kcal\,mol^{-1}}$ after the ZPE correction (Table 1). The comparison of the BSSE corrected binding energies shows that complex A is $5.2\,\mathrm{kcal\,mol^{-1}}$ more stable than complex B.

The third complex C shows the main interaction between one of the hydrogen atoms of water and the hydroxyl oxygen atom of formic acid. In addition, there is a weak secondary interaction between the formyl hydrogen atom of formic acid and the oxygen atom of water. The O–H · · · O–H hydrogen bond distance is 2.169 Å (MP2/aug-cc-pVTZ), and the C–H · · · O–H hydrogen bond distance is 2.478 Å. The uncorrected binding energy of complex C (MP2/aug-cc-pVTZ) is $-3.8\,\mathrm{kcal\,mol^{-1}}$, which is $1.7\,\mathrm{kcal\,mol^{-1}}$ less than that of complex B. The BSSE corrected binding energy is $-3.5\,\mathrm{kcal\,mol^{-1}}$, and the ZPE corrected binding energy is $-2.5\,\mathrm{kcal\,mol^{-1}}$. The binding energies obtained at the B3LYP/aug-cc-pVTZ and B3LYP/6-311++G(d,p) levels of theory are given in Table 2. To assign the additional peaks observed in the matrix spectra, structure and frequencies were computed for the 1:2 complex of formic acid with water. Minimum energy structures at the MP2/6-311++G(d,p), B3LYP/aug-cc-pVTZ and B3LYP/6-311++G(d,p) levels of theory (Fig. 6) resemble the structure reported by Priem et al. and Wei et al. [15,17].

4.3. Comparison of the calculated and experimental vibrational frequencies

The most perturbed vibrational mode in complex A is the O–H mode of formic acid, which is red shifted by $365\,\mathrm{cm^{-1}}$ at the MP2/aug-cc-pVTZ level of theory (Table 4). The other two vibrational modes of formic acid with marked shifts in complex A are the C=O ($-31\,\mathrm{cm^{-1}}$) and the C–O stretching vibration ($+90\,\mathrm{cm^{-1}}$). The frequency shifts of the symmetric stretching mode of water is −152, and that of the asymmetric stretching mode is $-49\,\mathrm{cm^{-1}}$ (MP2/aug-cc-pVTZ).

Table 2
Calculated DFT/B3LYP binding energies, raw and ZPE corrected (in $\mathrm{kcal\,mol^{-1}}$) of the formic acid–water complex

Complex	B3LYP/aug-cc-pVTZ		B3LYP/6-311++G(d,p)	
	ΔE	$\Delta E_{(\mathrm{ZPE})}$	ΔE	$\Delta E_{(\mathrm{ZPE})}$
A	−9.3	−6.8	−10.3	−7.8
B	−4.4	−2.8	−4.9	−3.3
C	−2.4	−1.2	−3.2	−1.9

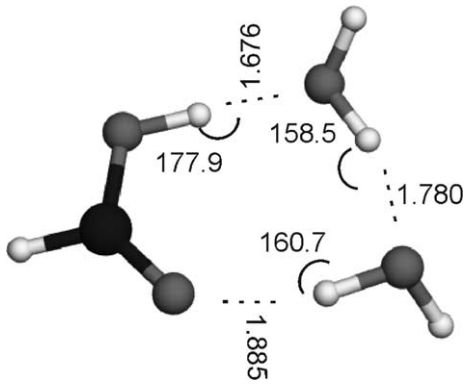

Fig. 6. The calculated structure (MP2/6-311++G(d,p)) of the 1:2 complex of formic acid–water, with hydrogen bond lengths (Å) and hydrogen bond angles (°).

On co-depositing formic acid and water in solid argon several new absorptions are observed which cannot be assigned to the parent species. These new bands appear close to the vibrational modes of formic acid and water. The perturbed modes of formic acid indicating the formation of a complex are found at 3212.4, 1736.7, and $1172.3\,\mathrm{cm^{-1}}$ as strong bands (Figs. 1–3). The corresponding parent modes are found at 3550.4 (O–H str.), 1767.1 (C=O str.), and $1103.5\,\mathrm{cm^{-1}}$ (C–O str.). The frequency shifts in the complex are thus −338, −30, and $+69\,\mathrm{cm^{-1}}$ for the O–H, C=O, and C–O stretching vibrations, respectively. The large red shift for the O–H stretching vibration indicates a strong interaction between formic acid and water. It is also evident that the carboxylic group of formic acid is the proton donor for the main interaction in this complex, as predicted by the calculations.

In the complex the symmetrical stretching mode of water at $3639.7\,\mathrm{cm^{-1}}$ exhibits a red shift of $103\,\mathrm{cm^{-1}}$, while the asymmetrical stretching mode at $3732.1\,\mathrm{cm^{-1}}$ is red shifted by only $40\,\mathrm{cm^{-1}}$. The frequency shift of the asymmetrical mode is small, which is commonly observed for a hydrogen bonded complex of water [8–10,12,40]. The calculated frequency shifts at the MP2/aug-cc-pVTZ level agree reasonably well with the experimentally observed frequency shifts (Table 3).

The experiments using D_2O confirm the assignment of the water modes in the formic acid−water complex. The symmetrical stretching mode of D_2O at $2657.7\,\mathrm{cm^{-1}}$ is red shifted to $2592.7\,\mathrm{cm^{-1}}$, and the asymmetrical stretching mode at $2771.0\,\mathrm{cm^{-1}}$ is red shifted to $2732.4\,\mathrm{cm^{-1}}$. The relative frequency shifts, $\Delta\nu/\nu$ ($\nu_{\mathrm{monomer}} - \nu_{\mathrm{complex}}/\nu_{\mathrm{monomer}}$) in the D_2O symmetrical ($\Delta\nu/\nu = 0.024$) and asymmetrical stretching mode ($\Delta\nu/\nu = 0.014$) agree well with that obtained in the H_2O experiment $\Delta\nu/\nu = 0.028$ and 0.011, respectively (Table 4).

The experimental infrared spectrum of the formic acid–water complex reasonably agrees with the calculated spectrum of complex A (Fig. 7). Only the O–H stretching vibration in the complex shows a larger deviation, in agreement with observations described in literature [41,42].

Table 3
The experimental (Ar matrix at 15 K) and the calculated (MP2) unscaled vibrational frequencies of the formic acid–water complex A, along with the frequency shift in the complex, $\Delta\nu$, from the isolated monomer (in parentheses)

Experimental frequencies (cm^{-1})		Computed frequencies (cm^{-1})				Mode of assignment
		MP2/aug-cc-pVTZ		MP2/6-311++G(d,p)		
Monomer	Complex	Monomer	Complex	Monomer	Complex	
3550.4	3212.4 (−338)	3740.8	3376.0 (−365)	3797.2	3507.1 (−290)	O–H-stretching (ν_1)[a]
1767.1	1736.7 (−30)	1793.7	1762.7 (−31)	1807.5	1782.6 (−25)	C=O-stretching (ν_3)[a]
1103.5	1172.3 (+69)	1130.9	1220.9 (+90)	1142.6	1219.9 (+77)	C–O-stretching (ν_6)[a]
3639.7	3536.8 (−103)	3822.0	3670.1 (−152)	3884.1	3801.1 (−83)	O–H-stretching (ν_1)[b]
3732.1	3692.0 (−40)	3947.8	3898.5 (−49)	4002.2	3964.5 (−38)	O–H-stretching (ν_3)[b]

[a] Formic acid fundamental modes in the complex.
[b] Water fundamental modes in the complex.

Table 4
Comparison of experimental (Ar matrix at 15 K) and calculated (MP2/6-311++G(d,p)) frequency shifts ($\Delta\nu/\nu$) of the formic acid–water and formic acid–D_2O complex A

Experimental		Computed		Mode of assignment
H_2O	D_2O	H_2O	D_2O	
0.028	0.024	0.021	0.021	O–H-stretching (ν_1)
0.011	0.014	0.010	0.011	O–H-stretching (ν_3)

Table 5
The experimental (Ar matrix at 15 K) and the calculated (MP2/6-311++G(d,p)and B3LYP) unscaled vibrational frequencies (in cm^{-1}) of the 1:2 formic acid–water complex, along with the frequency shift in the complex, $\Delta\nu$, from the isolated monomer (in parentheses)

Experimental frequencies	Computed frequencies			Mode of assignment
	MP2/6-311++G(d,p)	B3LYP/aug-cc-pVTZ	B3LYP/6-311++G(d,p)	
–	3273.7 (−524)	3023.5 (−694)	3109.4 (−629)	O–H- stretching (ν_1)[a]
1722.4 (−45)	1774.6 (−33)	1748.9 (−63)	1755.8 (−60)	C=O-stretching (ν_3)[a]
–	1261.6 (119)	1252.9 (132)	1253.1 (128)	C–O-stretching (ν_6)[a]
–	3597.9 (−286)	3393.6 (−400)	3447.8 (−369)	O–H-stretching (ν_1)[b]
3441.1 (−199)	3722.5 (−162)	3531.1 (−262)	3586.6 (336)	O–H- stretching (ν_1)[b]

[a] Formic acid fundamental modes in the complex.
[b] Water fundamental modes in the complex.

4.4. 1:2 Complex of formic acid–water

The frequency shift of the C=O stretching mode is predicted to $-33\,cm^{-1}$, and that of the O–H stretching mode of water bonded to the carbonyl oxygen atom to $162\,cm^{-1}$ at the MP2/6-311++G(d,p) level of theory (Table 5). Only these two modes are observed in the formic acid–water experiments. The experimental C=O stretching vibration is observed at $1722.2\,cm^{-1}$ which correspond to a red shift of −45 compared to formic acid. The O–H stretching vibration of water is found at $3441.1\,cm^{-1}$, corresponding to a red shift of $-199\,cm^{-1}$ compared to uncomplexed water. Thus, the experimental data are in reasonable agreement with the calculation.

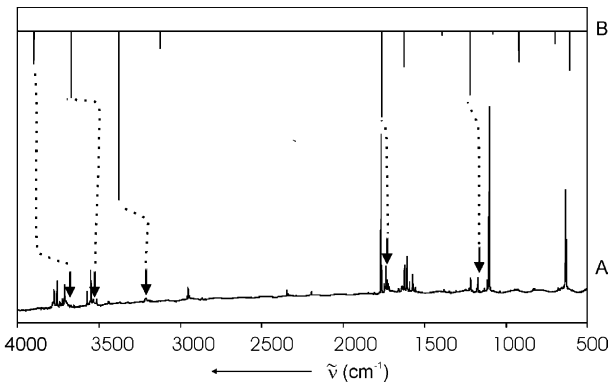

Fig. 7. Comparison of the matrix isolation infrared spectra of formic acid–water–Ar mixture with the computed spectra of the complex A: A, MP2/aug-cc-pVTZ; B, HCOOH–H_2O–Ar (1/1/1000) by supersonic jet sampling.

4.5. Comparison of the structural parameters and the frequency shifts

The extend of bond lengthening or shortening correlates very well with the amount of red or blue shifts observed in the corresponding vibrational modes on complex formation. The changes in the structural parameters of the monomers due to complex formation are reasonably large (Table 6). In the 1:1 complex the largest changes occur for the O–H and C–O bond of formic acid (r(O–H) is lengthened by 0.018 Å

Table 6
Comparison of the selected geometric parameters of the formic acid, water, and formic acid–water complex A[a]

	Parameters	MP2/aug-cc-pVTZ	MP2/6-311++G(d,p)
HCOOH	r(O–H)	0.971	0.969
	r(C–O)	1.347	1.348
	r(C=O)	1.205	1.205
	∠(COH)	106.45	106.34
	∠(O=CO)	125.11	125.20
H_2O	r(O–H)	0.961	0.960
	∠(HOH)	104.11	103.45
Complex A	r(O–H)^f	0.989	0.983
	r(C–O)	1.328	1.332
	r(C=O)	1.217	1.215
	∠(COH)	107.50	107.43
	∠(O=CO)	125.87	126.04
	r(O–H_1)^w	0.962	0.960
	r(O–H_2)^w	0.973	0.967
	r(O–$H^f \cdots$O)	1.768	1.793
	r(O–$H^w \cdots$O)	2.002	2.142
	∠(O–$H^f \cdots$O)	157.58	158.91
	∠(O–$H^w \cdots$O)	136.16	127.24

f: formic acid and w: water.
[a] The bond distances are given in Å and angles in degrees.

and r(C–O) shortened by 0.019 Å). This correlates nicely with the large frequency shifts of the O–H (towards red) and C–O (towards blue) stretching vibrations. The C=O bond is lengthened by 0.012 Å, and a similar lengthening is observed for the O–H of H_2O bonded to the C=O group. This is a clear evidence for the secondary interaction involving one of the hydrogen atoms of water and the carbonyl oxygen of formic acid giving rise to a cyclic structure.

5. Conclusions

The matrix isolation infrared spectra together with ab initio and DFT calculations have been used to characterize the 1:1 and 1:2 complexes of formic acid and water. Three stable 1:1 complexes with cyclic geometries were found using MP2 and DFT methods. The global minimum structure A has two strong O–H. . . O interactions with short hydrogen bonds. In the main interaction, contributing most to the binding of the complex, the formic acid functions as a proton donor and the water as a proton acceptor. The most convincing evidence for this main interaction is the large red shift of the O–H stretching vibration of the formic acid subunit ($-338\,cm^{-1}$). A large binding energy is always paralleled by large frequency shifts due to the complex formation. The BSSE corrected binding energy of the global minimum structure A is $-10.3\,kcal\,mol^{-1}$ (MP2/aug-cc-pVTZ). The other two structures show one O–H $\cdots$ O interaction and a weak C–H $\cdots$ O interaction, giving rise to a cyclic complex with a lower binding energy (-5.1 and $-3.5\,kcal\,mol^{-1}$ at the MP2/aug-cc-pVTZ after BSSE correction). Only the most stable complex was identified in the matrix experiments. Experiments with D_2O were carried out to confirm the assignment of the O–H stretching vibrations of water. The experimentally observed frequency shifts of the vibrational modes of formic acid and water induced by the complex formation are in reasonable agreement with the calculated values.

Acknowledgements

Financial support from the Deutsche Forschungsgemeinschaft (SFB 452) and the Fonds der Chemischen Industrie is gratefully acknowledged. We thank Dr. Holger Bettinger for fruitful discussions.

References

[1] P.R. Rablen, J.W. Lockman, W.L. Jorgensen, J. Phys. Chem. A 102 (1998) 3782.
[2] S. Aloisio, P.E. Hintze, V. Vaida, J. Phys. Chem. A 106 (2002) 363.
[3] P.G. Jasien, W.J. Stevens, J. Chem. Phys. 84 (1986) 3273.
[4] A. Nowek, J. Leszczynski, J. Phys. Chem. A 101 (1997) 3784.
[5] K. Sankaran, V. Vidya, K.S. Viswanathan, L. George, S. Singh, J. Phys. Chem. A 102 (1998) 2944.
[6] K.N. Kirschner, R.J. Woods, J. Phys. Chem. A 105 (2001) 4150.
[7] E.S. Kryachko, M.T. Nguyen, T. Zeegers-Huyskens, J. Phys. Chem. A 105 (2001) 1934.
[8] B. Nelander, J. Chem. Phys. 72 (1980) 77.
[9] X.K. Zhang, E.G. Lewars, R.E. March, J.M. Parnis, J. Phys. Chem. 97 (1993) 4320.
[10] A. Engdahl, B. Nelander, P. Astrand, J. Chem. Phys. 99 (1993) 4894.
[11] L. George, K. Sankaran, K.S. Viswanathan, C.K. Mathews, Appl. Spectrosc. 48 (1994) 7.
[12] A. Givan, H. Grothe, A. Loewenschuss, C. Nielsen, J. Phys. Chem. Chem. Phys. 4 (2002) 255.
[13] P.O. Astrand, G. Karlstrom, A. Engdahl, B. Nelander, J. Chem. Phys. 102 (1995) 3534.
[14] G. Velardez, J.L. Heully, J.A. Beswick, J.P. Daudey, Phy. Chem. Comm. 6 (1999) 24.
[15] D. Priem, T. Ha, A. Bauder, J. Chem. Phys. 113 (2000) 169.
[16] R. Liftimie, D. Salahub, D. Wei, J. Schofield, J. Chem. Phys. 113 (2000) 4852.
[17] D. Wei, J. Truchon, S. Sirois, D. Salahub, J. Chem. Phys. 116 (2002) 6028.
[18] M.J. Frisch, G.W. Trucks, H.B. Schlegel, G.E. Scuseria, M.A. Robb, J.R. Cheeseman, V.G. Zakrzewski, J.A. Montgomery, R.E. Stratmann, J.C. Burant, S. Dapprich, J.M. Millam, A.D. Daniels, K.N. Kudin, M.C. Strain, O. Farkas, J. Tomasi, V. Barone, M. Cossi, R. Cammi, B. Mennucci, C. Pomelli, C. Adamo, S. Clifford, J. Ochterski, G.A. Petersson, P.Y. Ayala, Q. Cui, K. Morokuma, D. K. Malick, A.D. Rabuck, K. Raghavachari, J.B. Foresman, J. Cioslowski, J.V. Ortiz, B.B. Stefanov, G. Liu, A. Liashenko, P. Piskorz, I. Komaromi, R. Gomperts, R.L. Martin, D.J. Fox, T. Keith, M.A. Al-Laham, C.Y. Peng, A. Nanayakkara, C. Gonzalez, M. Challacombe, P.M. W. Gill, B.G. Johnson, W. Chen, M.W. Wong, J.L. Andres, M. Head-Gordon, E.S. Replogle, J.A. Pople, Gaussian 98 (Revision A.11), Gaussian Inc., Pittsburgh, PA, 2001.
[19] C. Møller, M.S. Plesset, Phys. Rev. 46 (1934) 618.
[20] A.D. Becke, J. Chem. Phys. 98 (1993) 5648.
[21] C. Lee, W. Yand, R.G. Parr, Phys. Rev. B 37 (1988) 785.
[22] R. Krishnan, J.S. Brinkley, R. Seeger, J.A. Pople, J. Chem. Phys. 72 (1980) 650.
[23] M.J. Frisch, J.A. Pople, J.S. Brinkley, J. Chem. Phys. 80 (1984) 3265.

[24] T.H. Dunning Jr., J. Chem. Phys. 90 (1989) 1007.
[25] S.F. Boys, F. Bernardi, Mol. Phys. 19 (1970) 553.
[26] I.D. Reva, A.M. Plokhotnichenko, E.D. Radchenko, G.G. Sheina, Yu.P. Blagoi, Spectrochim. Acta A 50 (1994) 1107.
[27] J. Lundell, M. Räsänen, Z. Latajka, Chem. Phys. 189 (1994) 245.
[28] R.L. Redington, J. Mol. Spectrosc. 65 (1977) 171.
[29] M. Pettersson, J. Lundell, J. Am. Chem. Soc. 119 (1997) 11715.
[30] M. Halupka, W Sander, Spectrochim. Acta A 54 (1998) 495.
[31] M. Gantenberg, M. Halupka, W. Sander, Chem. Eur. J. 6 (2000) 1865.
[32] R.L. Redington, D.E. Milligan, J. Chem. Phys. 37 (1962) 2162.
[33] R.L. Redington, D.E. Milligan, J. Chem. Phys. 39 (1963) 1276.
[34] G.P. Ayers, A.D.E. Pullin, Chem. Phys. Lett. 29 (1974) 609.
[35] G.P. Ayers, A.D.E. Pullin, Spectrochim. Acta A 32 (1976) 1629, 1641.
[36] R.M. Bentwood, A.J. Barnes, W.J. Orville-Thomas, J. Mol. Spectrosc. 84 (1980) 391.
[37] J.P. Perchard, Chem. Phys. 273 (2001) 217.
[38] J. Lundell, M. Räsänen, J. Phys. Chem. 99 (1995) 14301.
[39] S. Tsuzuki, H. Houjou, Y. Nagawa, K. Hiratani, J. Phys. Chem. A 104 (2000) 1332.
[40] J. Sadlej, R. Moszynski, J.Cz. Dobrowolski, A.P. Mazurek, J. Phys. Chem. A 103 (1999) 8528.
[41] G.M. Chaban, J.O. Jung, R.B. Gerber, J. Phys. Chem. A 104 (2000) 2772.
[42] Z. Latajka, Z. Mielke, A. Olbert-Majkut, R. Wieczorek, K.G. Tokhadze, Phys. Chem. Chem. Phys. 1 (1999) 2441.